UDK 669.14.018.583:620.179.11:543.428.2
Izvirni znanstveni članek

ISSN 1580-2949
MTAEC 9, 36(6)313(2002)

AN ANALYSIS OF CROSS-SECTIONS OF ELECTRICAL STEELS WITH AN OXIDE LAYER

ANALIZA PREČNIH PREREZOV ELEKTROPLOČEVIN Z OKSIDNO PLASTJO

Djordje Mandrino, Matjaž Godec, Nataša Lipovšek, Monika Jenko

Institute of Metals and Technology, Lepi pot 11, 1000 Ljubljana, Slovenia
djordje.mandrino@imt.si

Prejem rokopisa - received: 2002-11-12; sprejem za objavo - accepted for publication: 2002-12-02

Non-oriented electrical steels are annealed at high temperatures during the manufacturing process in a gas mixture of hydrogen, nitrogen and water vapour to achieve decarburization and recrystallization. A complex oxide layer approximately several μm thick is formed on the surface of the electrical steel in the course of this thermal treatment. An analysis of the upper surface of the oxide layer provides information about this very surface - if the surface sensitive probe is used, or, alternatively, the information that is averaged over the whole thickness of the oxide layer is obtained. Therefore, a cross-section of an electrical steel with an oxide layer was analysed using high-resolution Auger electron spectroscopy (HRAES). The oxide layer is extremely brittle and can be very easily peeled off the electrical steel. This is why the usual metalographic method of preparing the cross-section of the sample by mounting the electrical steel in epoxy or some other non-conducting organic material may prove to be difficult. Such a material has to be removed before introducing the sample into the UHV chamber of the analysing equipment which often destroys the sample. Several techniques including using a low-melting-point Pb-Bi-In-Sn alloy to produce the cross-sections were employed.

Key words: electrical steels, cross-section, HRAES, surface, oxide layer, low-melting-point alloy

Neorientirane elektropločevine v procesu izdelave zaradi razogljičenja in rekristalizacije žarimo v plinski mešanici vodika, dušika in vodne pare pri visokih temperaturah. Pri tem se na površini elektropločevine tvori kompleksna oksidna plast debeline nekaj μm. Z analizo površine oksidne plasti dobimo bodisi informacijo prav o tej površini, če uporabljamo površinsko občutljivo analizno tehniko, ali pa informacijo povprečeno čez celo debelino oksidne plasti. Zato smo se odločili za analizo prečnega prereza elektropločevine in oksidne plasti z visokoločlivo spektroskopijo Augerjevih elektronov (HRAES). Pri tem se je pojavila težava pri pripravi vzorca - oksidna plast je namreč zelo krhka in se z lahkoto lušči z elektropločevine. Navadna metalografska priprava prečnega prereza z vročim ali hladnim zalivanjem vzorca v neprevoden organski material lahko povzroča težave, saj je treba tovrsten material pred vnosom vzorca v UVV analizno aparaturo odstraniti, pri čemer je vzorec pogosto uničen. Preizkusili smo različne načine priprave prečnega prereza, med drugim zalivanje vzorca v nizkotaljivo zlitino na osnovi Pb-Bi-In-Sn.

Ključne besede: elektropločevine, prečni prerez, HRAES, površina, oksidna plast, nizkotaljiva zlitina

1 INTRODUCTION

The composition of the oxide layer on the surface of electrical steels is very important from the technological point of view. Normally, its composition reflects the manufacturing process. Non-oriented electrical steels may be alloyed with Si and Al in order to increase their electrical resistivity. Also, traces of elements such as Cu and S (so-called "tramp elements") and their compounds may be found in the final product because electrical steels are manufactured from scrap steel.

In the course of the manufacturing process the electrical steel is hot rolled, then cold rolled and finally decarburised and recrystallized in a gas mixture of N_2 + H_2 + $(H_2O)_g$. During the decarburisation process a surface oxide layer is formed. This layer, apart from its principal components, often contains trace elements in various forms

So far surface spectroscopies have frequently been used to study oxide layers on metal surfaces (e.g. [1, 2, 3]). This particular material has already been studied in our lab by XPS and HRAES [4, 5, 6]. However, different studies of basically identical materials with minor differences in the thermal treatment revealed some differences in the oxide layer composition that are likely to appear due to the analysis technique as well as due to some differences in the samples' treatment. XPS and most of the AES in [4, 6] were performed over wide areas thus yielding averaged results of the oxide layers' elemental composition and masking possible inhomogenities in the plane of the sample (inhomogenities perpendicular to this plane were, however, already established in [4]). In [5] the oxide layer was probed locally by HRAES, establishing relatively high Al concentrations in isolated, small compact areas. These areas were still contributing to a very low overall Al concentration. The analyses in this study were undertaken in order to add to our understanding of the composition of the oxide layers of electrical steels, especially with respect to in-depth inhomogenities and their dependence on thermal thermal treatments carried out prior to the analysis.

2 EXPERIMENTAL

In the course of the manufacturing process the electrical steel used for preparing the samples was

alloyed with 2% of Si and 1% of Al, and subsequently hot and cold rolled to produce sheets of 0.5 mm thickness. These sheets were cut into platelets of approximately 90 mm × 20 mm. Decarburisation and recrystallization were carried out under laboratory conditions by annealing the samples in a gaseous mixture of N_2 + H_2 + $(H_2O)_g$. From one to three annealing cycles were then performed. The parameters of these cycles for the individual samples are given in **Table 1**.

Table 1: Decarburization thermal treatment parameters for the samples studied
Tabela 1: Parametri dekarburizacijske toplotne obdelave za preiskovane vzorce

Sample	T_1 (°C)	T_2 (°C)	T_3 (°C)	$H_2 : N_2$	t_1 (min)	t_2 (min)	t_3 (min)
A	840	970	1040	25 : 75	3	1	1
B	970			30 : 70	5		
C	840	950		30 : 70	2	2	
D	840		950	30 : 70	5		5

After the thermal treatment smaller platelets of approximately 10 mm × 15 mm were cut out and prepared for an AES analysis of the cross section. Since the oxide layer is extremely brittle and can be very easily peeled off in scales of different (sub-milimeter) sizes, various techniques for preparing the cross-section of the sample were employed. Conventional mounting of the sample into epoxy and polishing the lateral surface had the disadvantage that in most cases when the epoxy was removed from the sample, most of the oxide layer was also removed. A low-melting-point Pb-Bi-In-Sn alloy, unlike epoxy, could be introduced into the UHV; however, the cross-section/alloy interface proved to be somewhat blurred, the oxide layer being, in some cases, completely covered with the alloy due to the polishing. The most useful method proved to be simply mounting a piece of peeled-off scale of the oxide layer into a molten drop of the Pb-Bi-In-Sn alloy. This was a somewhat tedious job that was accomplished with a pair of tweezers and a magnifying glass.

VG Microlab 310F apparatus with a base vacuum during the analysis below 10^{-9} mbar was used to image the surface of the samples as well as to record the AES and HRAES linescan spectra. The Auger spectra of the samples showed very intense carbon and oxygen peaks, and Fe peaks of very low intensity. Therefore, before any further analysis the surface of the sample was cleaned by argon sputtering using a 3 keV ion energy and a 1 μAcm^{-2} current density for 15 minutes in order to remove layers of adsorbed impurities and to expose the bare oxide layer that had been produced during the sample preparation process. Intense carbon and oxygen peaks were also found on the cross-sections, so these were also cleaned by argon sputtering prior to measuring the linescans. The AES measurements were performed at an electron beam energy of 10 keV, the same as used for the SEM imaging. The SEM images and the AES and XPS spectra were processed with the Eclipse Data System v2.1 software package.

3 RESULTS AND DISCUSSION

A typical SEM image of sample A is shown in **Figure 1**. On the micrometer scale the surface is highly corrugated. An Auger spectrum in **Figure 2**, acquired from the area in **Figure 1** shows clearly that an iron oxide is the dominant component of the layer. Note, also, the presence of the small peaks of C, Al and Si Auger electrons. A SEM image of a somewhat larger surface area of sample B, where two distinct types (compact and porous) of the oxide layer can be distinguished, is shown in **Figure 3**. The corresponding Auger spectra from the points P1-P3, presented in **Figure 4**, show that these two oxide-layer types mainly differ in their aluminium content. One can also notice that Si Auger electron peaks

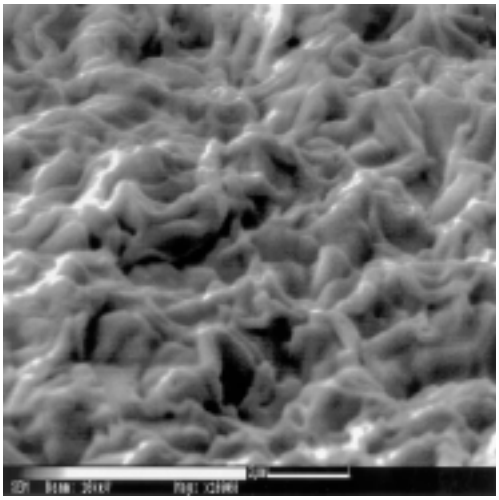

Figure 1: SEM image of the surface-oxide layer in sample A
Slika 1: SEM-posnetek površinske oksidne plasti vzorca A

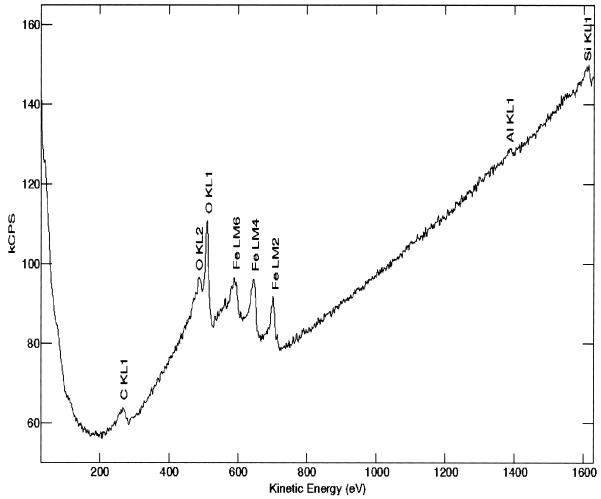

Figure 2: Survey AES spectrum of the area shown in **Figure 1**
Slika 2: Pregledni AES-spekter območja s **slike 1**

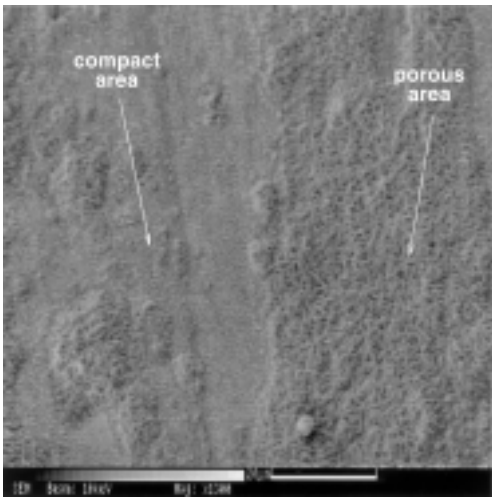

Figure 3: SEM image of the surface-oxide layer with porous and compact area in sample B

Slika 3: SEM-posnetek površinske oksidne plasti z dvema različnima tipoma površine

are almost undetectable in the spectra from P1-P3. This suggests that while the large-scale composition of the oxide layer is of the ferrous oxide type, the concentration of the lesser components varies substantially over the oxide surface.

To observe the variation of these concentrations with the depth of the oxide layer several AES linescans were performed by measuring Auger spectra at 20 to 30 points along selected lines on the cross-sections of the samples A, C and D.

30 points were measured along the line L1 (**Figures 5a, 5b**) in sample A. The concentration profiles for Fe, O and Si calculated from these spectra showed that the Si concentration was highest at a depth near the oxide layer/metal interface, but still not with a very high

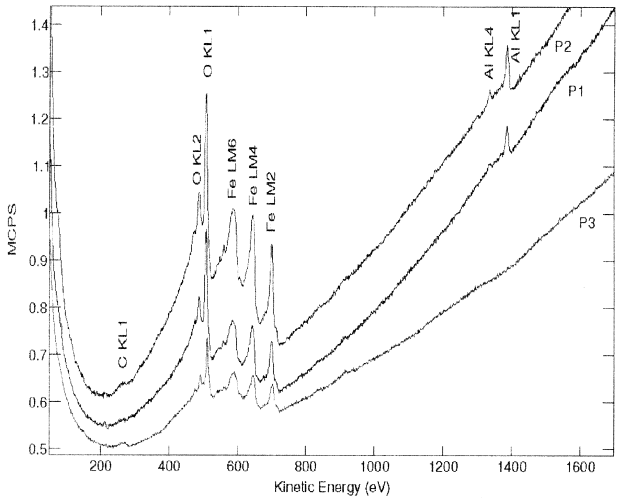

Figure 4: AES spectra from the area shown in Figure 3. P1 and P2 were acquired from the compact part of the area and P3 in the porous part.

Slika 4: AES-spektri območja s slike 3. P1 in P2 sta bila merjena v kompaktnem, P3 pa v poroznem področju.

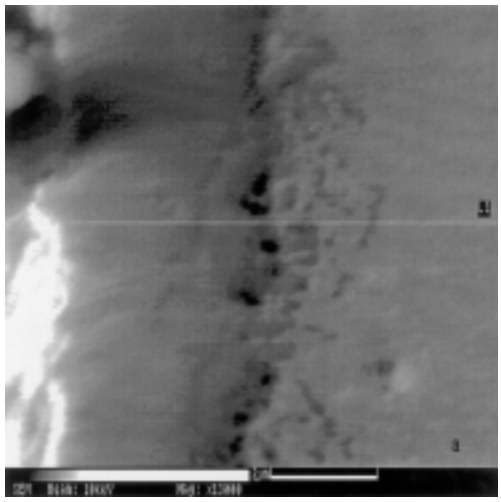

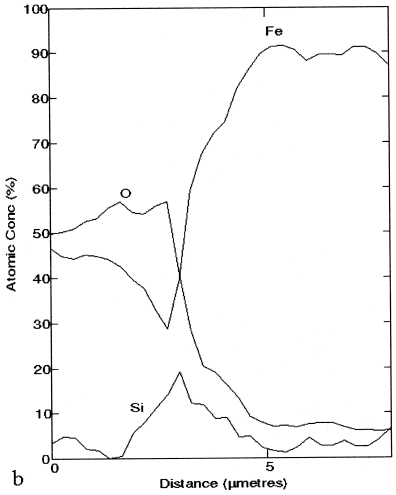

Figure 5: SEM image of the cross-section of the oxide-layer/metal interface in sample A (a); Fe, Si and O atomic concentrations along the line L1 (b)

Slika 5: SEM-posnetek stika med oksidno plastjo in kovino v prerezu pri vzorcu A (a); atomske koncentracije Fe Si in O vzdolž črte L1 (b)

absolute value, and a maximum at approximately 20 at.%, which suggested that the concentration of any Si compound was also much higher in that region than on the surface. This is consistent with the low surface concentration of Fe_2SiO_4 measured in this sample by XPS (see [4]) as well as with the low intensity of the Si Auger electron peaks in the Auger spectrum in **Figure 2**. It is also known that electrical steels alloyed with approximately 2 % of Si are expected to produce Fe-Si-O compounds in the oxide layers on the surface [7, 8, 9].

25 and 20 points were measured along the lines L1 and L2 (**Figures 6a, 6b, 6c**) in sample C. Separate linescans were performed since, unlike the previous measurement, in this case the oxide layer was well detached from the surface thus forming a deep gap at the oxide layer/metal interface. The intensity of the Auger electron signal from this gap was greatly diminished.

In **Figure 6b** the profiles for Fe and O in the metal show nearly constant concentrations for both elements

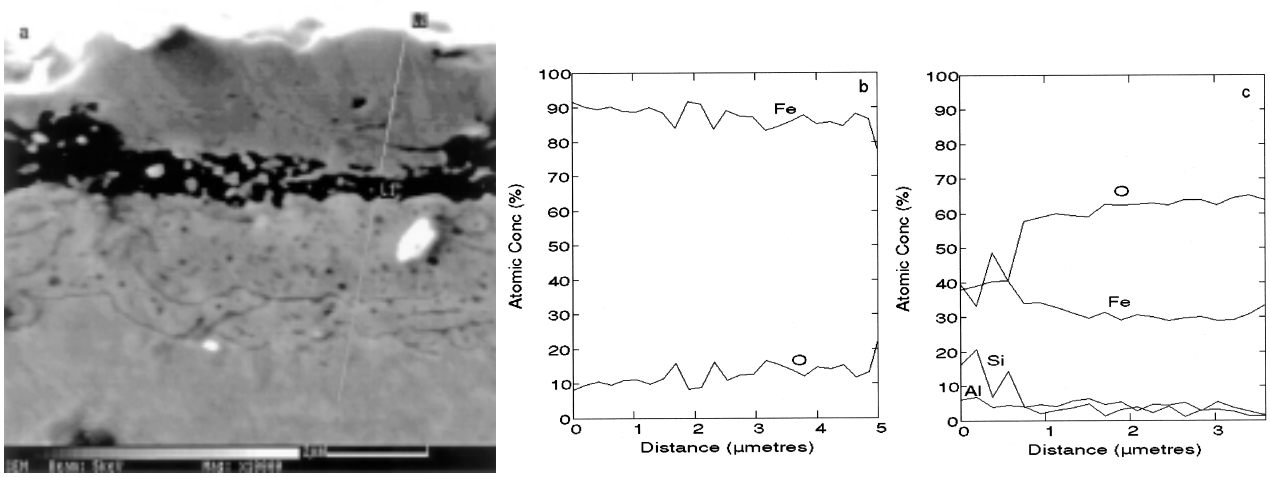

Figure 6: SEM image of the cross-section of the oxide-layer/metal interface in sample C (a); Fe and O atomic concentrations along the line L1 below the interface (b); Fe, Al, Si and O atomic concentrations along the line L2 in the oxide layer (c)
Slika 6: SEM-posnetek stika med oksidno plastjo in kovino v prerezu pri vzorcu C (a); atomske koncentracije Fe in O vzdolž črte L1 pod mejno ploskvijo (b); atomske koncentracije Fe, Al, Si in O vzdolž črte L2 v oksidni plasti (c)

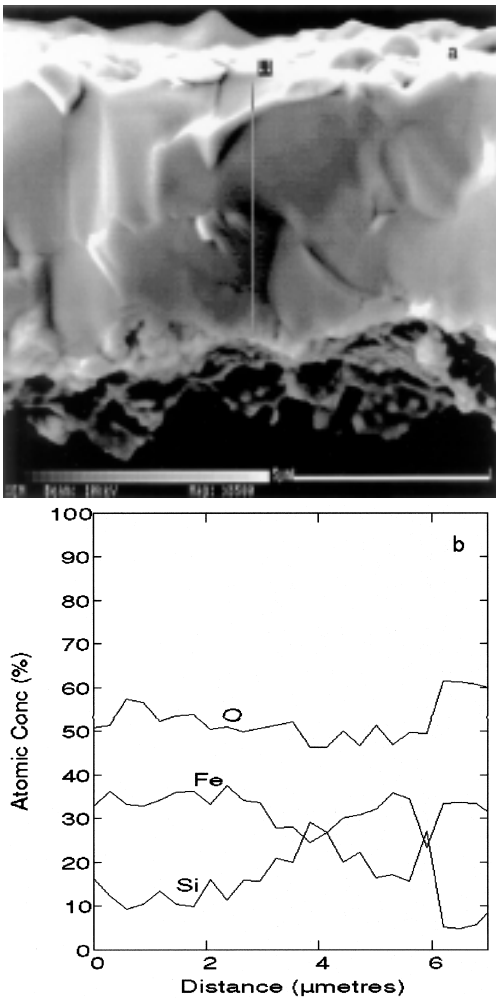

Figure 7: SEM image of the lateral surface of the oxide layer in sample D (a); Fe, Si and O atomic concentrations along the line L1 (b)
Slika 7: SEM-posnetek stranske ploskve oksidne plasti pri vzorcu D (a); atomske koncentracije Fe Si in O vzdolž črte L1 (b)

with the O concentration at relatively low value and increasing very slowly. Only at the very edge of the metal does the concentration of O suddenly increase, but this may also be attributed to some submicron-sized leftover from the oxide layer remaining attached to the metal. In the spectra that were used to construct the profiles in **Figure 6b** neither Si nor Al Auger peaks appeared. In **Figure 6c** the profiles for Fe, O as well as Si and Al are presented. There is some similarity with profiles in **Figure 5b** on the oxide-layer part of the oxide layer/metal interface: it is noticable that Si (and Al) concentrations close to the interface (gap) decrease rapidly when going towards the surface of the oxide, while simultaneously the O and Fe concentrations reach values approximately corresponding to a ferrous oxide stochiometry (Fe_2O_3 or Fe_3O_4 [4, 5, 6]). Since the basic material is the same in all samples it can be argued that Si is promoted into the oxide layer to form an Fe-Si-O compound that is again expected [6, 7, 8]. Total depletion of the Si in the metal layer below the metal/oxide layer interface may be due to this promotion. The relatively low average concentrations of the Fe-Si-O and/or Fe-Si-Al compounds in the oxide layers of samples A, C and B found in [4, 5] and [6] may be due to the somewhat non-standard parameters of the decarburization thermal treatments used for these samples [10].

25 points were measured along the line L1 in sample D (**Figures 7a, 7b**). Since this sample consisted of the peeled-off scale of the oxide layer mounted into the low-melting-point alloy the linescan could be performed over the oxide layer only.

Unlike previous linescans this one gives a relatively high concentration of silicon (cca 20 at.%) throughout the thickness of the oxide layer, but in the uppermost area it drops to below 10 at.%. The concentrations of Fe and O are again consistent with a ferrous oxide of the

Fe_3O_4 or Fe_2O_3 type. A possible reason for this difference in the distribution of Si (but also Fe and O, since their distibution only slightly changes over the measurement range, which is not the case with other samples) with respect to its distribution in samples A and C may be in the different thermal treatment of sample D, which lasted approximately twice as long as for the other two samples (**Table 1**).

4 CONCLUSIONS

SEM, HRAES and linescan cross-sectional analyses of electrical steel samples with oxide layers formed during the decarburization process were performed. The analyses yielded somewhat different results depending on the parameters of the decarburization thermal treatments. Ferrous oxides of approximately Fe_2O_3 or Fe_3O_4 stoichiometries were found in all samples. The upper surfaces of the oxide layers were very corrugated, as in sample A, or porous with included more compact areas, as in sample B. The linescan cross-sectional analyses showed that the diffusion of Si, and in some cases Al, over the metal/oxide-layer interface occurred during the decarburization thermal treatment and that the intensity of this diffusion is dependent on the parameters of the thermal treatment.

5 REFERENCES

[1] Lee YP, Bevolo AJ Lynch DW. Surf. Sci.; 188, (**1987**) 267
[2] Carriere B, Deville JP, Brion D, Escard J. Electr. Spectr. Relat. Phen.; 10 (**1977**) 85
[3] Hughes AE. Corrosion Sci.; 22 (**1982**) 103
[4] Mandrino Dj, Jenko M, Prešeren V. Kovine Zlitine Tehnologije; 33 (**1999**) 419
[5] Mandrino Dj, Jenko M. Vacuum; 61 (**2001**) 157
[6] Lipovšek N, Jenko M, Breskvar B, Koroušič B, Kosec L, Prešeren V. Mater. Tehnol. 35 (**2001**) 381
[7] Eckstein HJ. Technologie der Waermebehandlung von Stahl. VEB Deutcher Verlag fuer Grundstoffindustrie, Leipzig, 1987
[8] Peters FK, Engell HJ. Arch. Eisenhuettenwess.; 30 (**1959**) 275
[9] Schreir LL, Jarman RA, Burstein GT. Corrosion, Vol. 1, Metal/ Environment Reactions, Butterworth-Heinemann, Oxford, 1995
[10] Steiner Petrović D, Jenko M, Gontarev V, Grabke HJ. Kovine Zlitine Tehnologije; 32 (**1998**) 493